

# Ignition Behavior of Marine Diesel Sprays

Investigation of Marine Diesel Ignition and Combustion at Engine-Like Conditions  
by means of OH\* Chemiluminescence and Soot Incandescence

\*Andreas Schmid, Beat von Rotz, Rolf Bombach<sup>+</sup>, German Weisser, Kai Herrmann  
and Konstantinos Boulouchos<sup>++</sup>

*Wärtsilä Switzerland Ltd.  
Zürcherstrasse 12, CH-8404 Winterthur, Switzerland*

*<sup>+</sup>Paul Scherrer Institute, PSI  
CH-5232 Villigen PSI, Switzerland*

*<sup>++</sup>ETH Zürich  
Sonneggstrasse 3, CH-8092 Zürich, Switzerland*

*Key Words:* Marine Diesel, Combustion, Experiments, Diagnostics, Chemiluminescence

## ABSTRACT

In this contribution, an initial investigation of the ignition behavior of large two-stroke marine diesel sprays has been performed. At engine-like conditions, the OH radical was traced with an intensified high speed camera and a sophisticated optical setup. A series of spectroscopic measurements showed, however, that the soot incandescence strongly contributes to the UV signal, superimposing with or even masking the chemiluminescence of the OH radical. As the combustion of typical fuels used in large two-stroke engines involves the formation of non-negligible amounts of soot, the signal is almost omnipresent during the oxidation process. A differentiation between the UV-light emitted by the OH radical and the UV-light emitted by soot incandescence is only possible when both signals are measured separately. Therefore, a second high speed camera recorded the light coming from soot incandescence. In addition, it recorded the background illuminated spray plume to make an exact positioning of the OH\* signal relative to the spray possible. A comparison of the two images then allowed the differentiation between the two light sources. In a first measurement series, which included a temperature variation, ignition delay, ignition location and flame lift-off have been measured. The results are in accordance with literature, as they show a dramatic decrease in ignition delay towards higher gas temperature. On the other hand the standard deviation increases towards lower gas temperatures. The ignition location and lift-off showed similar behavior: Lower gas temperature corresponds to an increase of the distance between ignition location/lift-off and nozzle orifice along with increased standard deviation. It could be shown that the applied technique works for the investigation of large marine diesel engine combustion systems.

## INTRODUCTION

The global ecological changes have triggered actions at various levels and big efforts have been made towards reducing the environmental impact of human activities in many sectors. In recent years, also shipping has come more and more into the focus of legislative bodies, resulting in the introduction and further development of the MARPOL Annex VI [1]. This regulation aims at limiting the emissions of pollutants such as NO<sub>x</sub>, SO<sub>x</sub> and particulate matter as well as at the further enhancement of the

efficiency of marine transport in order to minimize the CO<sub>2</sub> output. As a consequence, the priorities in the development of power systems in this sector are eventually changing and a considerably more thorough optimization is required. This can only be achieved on the basis of an in-depth understanding and profound knowledge of the processes related to combustion in marine diesel engines. Investigations of the injection process, mixture formation, ignition behavior and combustion characteristics at conditions representative of such combustion systems are required for establishing the necessary insight into these

highly complex in-cylinder phenomena of large two-stroke marine diesel engines. Finally, this enables and expedites the optimization and development of concepts and solutions for efficient diesel combustion. Furthermore, the acquisition of fundamental reference data with regard to spray and combustion characteristics is an absolute prerequisite for the further development of computational fluid dynamic (CFD) tools to assist the marine diesel engine combustion system design [2].

The Spray Combustion Chamber (SCC) represents a marine diesel engine-like combustion system, which has been developed [3] and operated within the framework of HERCULES (High-Efficiency R&D on Combustion with Ultra Low Emissions for Ships), a large scale research project [4] funded under the EC's Framework Programs. The experimental setup enables investigations and observations of in-cylinder processes at relevant conditions (up to 20 MPa peak firing pressure) such as fuel spray morphology and evaporation, ignition behavior, combustion and subsequently, emission formation. Furthermore, the fuel admission of a variety of different fuels including residual fuel types (heavy fuel oil) is realized by an engine-like injection system (common rail, pressure up to 120 MPa). The injected fuel can be observed under reactive as well as non-reactive (nitrogen) chamber conditions [5]. A wide range of combustion diagnostics techniques can be applied, thereby making use of the extensive optical accessibility via sapphire windows of 100 mm and 150 mm clear diameter.

The mixture formation and the ignition process are essential features of combustion and the subsequent pollutant formation in diesel engines. Therefore, after extensive investigations on the spray morphology and the fuel/air mixture [6]-[8] for a wide range of gas conditions as well as fuel qualities, initial experiments have been performed to better understand the phenomena related to the ignition and start of combustion of the injected diesel fuel spray.

The auto-ignition process in a diesel engine is a highly complex process with physical as well as chemical sub-processes starting with the fuel injection. This can be noticed by a significant rise of the pressure or emissions of natural light radiation. These light emissions, so called chemiluminescence [9], [10] originate from excited states of specific molecules formed by exothermic chemical reactions that occur primarily during stoichiometric combustion of typical hydrocarbon fuels. The OH\* chemiluminescence is an excellent marker for the temporal and spatial location of the initial combustion reactions. During the subsequent combustion, soot is created whose luminosity arises from the thermal or gray-body emission caused by soot particles heated up almost to the flame temperature of the combustion process [10].

In this contribution we present an initial investigation of the ignition behavior and the combustion of fuel

sprays relevant for large two-stroke marine diesel engines using OH\* chemiluminescence and simultaneous back illuminated imaging measurements [10]. The significance of the OH\* chemiluminescence measurements is proven by spectroscopic analysis of the emitted flame light of the combustion. Measurements were made at a variation of temperatures while gas density was kept constant in order to establish the influence on ignition delay and ignition. Furthermore, the flame lift-off as the most upstream location of fully established combustion has been determined.

## EXPERIMENTAL SETUP

Figure 1 shows the schematic principle of the Spray Combustion Chamber. In two high pressure bottles the gas – air or nitrogen – is compressed up to 320 bar. To pressurize the combustion chamber, the inlet valves open and the cold gas passes the regenerator. Its big surface heats up the gas before entering the chamber via the inclined inlet port. As a consequence of the tilted intake a strong swirl is generated, as it is typical for large two-stroke engines. After the experiment the outlet valve opens and releases the filling into the exhaust.

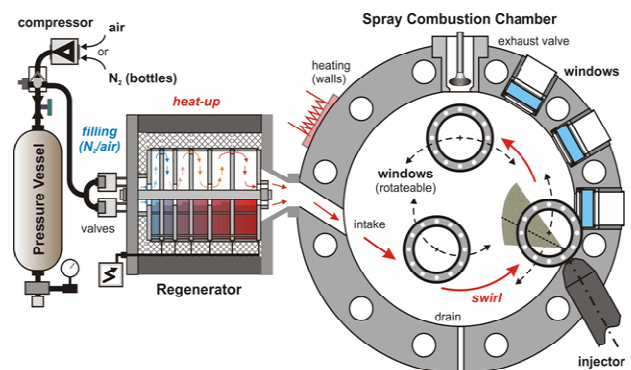


Fig. 1 Schematic principle of the experimental setup, exemplifying the operational (filling, heat up, swirl, injection) and functional aspects (window position, exhaust valve).

The dimension of the optically accessible constant volume chamber is representative for smaller two-stroke as well as larger four-stroke marine diesel engines ( $\varnothing$  500 x 150 mm). At start of injection, realistic operating conditions are achieved in terms of cylinder pressures, gas temperature and swirl [11]. The SCC allows large optical access through sapphire windows ( $\varnothing$  100 - 150 mm) which can be positioned at several locations to investigate large sprays.

For the present work, the following setups have been applied to investigate the ignition behavior of large marine diesel sprays. For the spectral investigation of light emitted by the combustion, a spectrometer (ARC SpectraPro-300i) has been combined with a LaVision high speed image intensifier (IRO) and a HSS6 high speed camera. Fig. 2 shows the setup in front of the SCC. A dichroic mirror (UV-guard) in front of the window reflects the UV light into the spectrometer while the visible and the infrared light are transmitted. With a

UV-objective (UV-Nikkor), the light is collected and focused onto the entrance slit of the spectrometer.

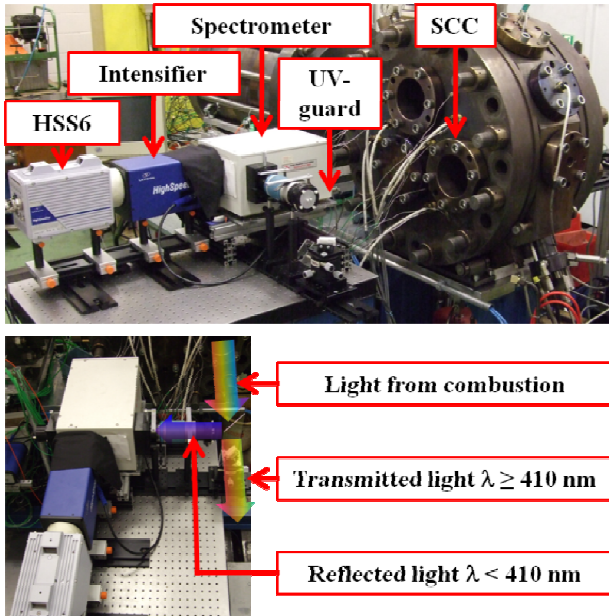


Fig. 2 Setup for spectral analysis

Based on the results and observations of the spectral analysis the setup shown in Fig. 3 was built up. Similar to the previous setup it consists of a UV mirror which separates the UV light from the visible light. The light from the OH\* is directed through a narrow band pass filter (313 nm, FWHM 10 nm) and a UV objective, into the LaVision high speed image intensifier (IRO). Visible and infrared light is transmitted through the mirror and filtered with a narrow band pass filter (689.1 nm, T60%, FWHM 10.6 nm), before recorded with a second HSS6 camera.

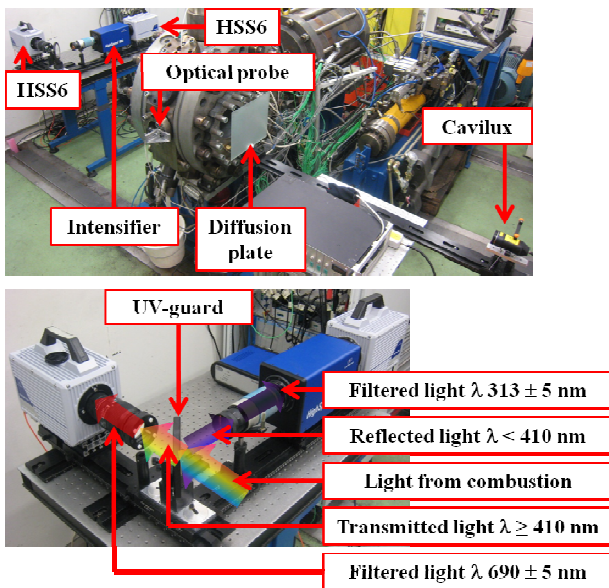


Fig. 3 Setup for simultaneous investigation of OH\* chemiluminescence and back illuminated images / soot incandescence  
To visualize the spray by means of back illumination

[12] the setup was additionally equipped with a Cavilux laser diode (690 nm) in combination with a diffusing plate as described in [6]. For both setups the frame rate of the cameras was set to 16 kHz.

The intensifier was driven with 90% gain and a gating of 50  $\mu$ s. For the spectral investigations the image size was set to 1024 x 368 pixels. For calibration the setup was tested and configured using a mercury arc lamp. With the help of the mercury's distinct spectra, the spectral resolution of the setup was determined. The two local maxima at 313.1 nm and 435.8 nm were imaged with a distance of 279 pixels what results in a horizontal resolution of 0.44 nm/pixel. The vertical axis was left in pixel, it represents the vertical position of the emitting object.

For simultaneous measurements of chemiluminescence and soot incandescence the image size was set to 512 x 512 pixels. In combination with the two 105 mm objectives a resolution of 0.292 mm/pixel could be achieved in both cases.

Furthermore, an optical probe [13] has been used to detect UV light around 313 nm. With a similar optical arrangement as for the camera on the UV path, the light within the combustion chamber has been recorded and was used to detect start of combustion. A detailed description of the optical arrangement behind the probe is discussed in [14].

## RESULTS AND DISCUSSIONS

Fig. 4 shows an image of the spectra of the early combustion. The horizontal axis reaches from about 270 nm on the left to 370 nm on the right. Conspicuous are the two stripes starting on the right hand side slowly fading towards the left side of the image. These two stripes represent the spectra of two burning spots. Their vertical position represents the real expansion in vertical direction. On the lower half no evidence of radiation can be seen. This is the region above the nozzle where no flame is expected. The lower, stronger spot is burning very bright already. Its intensity towards the longer wavelength is very high already, whereas its tail reaches almost down into the UV-B range. On closer examination one can note that even at the very beginning of the combustion, the luminescence signal is already dominated by incandescence of burning soot.

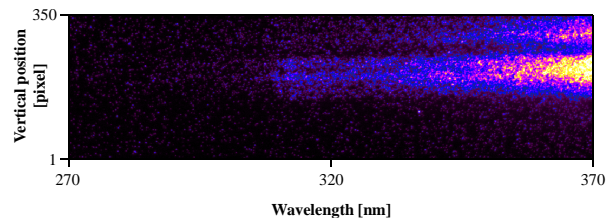


Fig. 4 Camera signal recorded after passing the spectrometer. The vertical axis depicts actual vertical position of the observed luminescence. The horizontal axis represents the spectral distribution of the signal. The image is centered on a wavelength of 320 nm.

Unfortunately, due to the high temperature of the

soot of 2000-2500 K, a significant part of the emitted radiation arises in the UV region of the spectrum, hence superimposing with or even masking the chemiluminescence of the OH radical. In order to assess this impact, a spectral analysis has been performed. For this purpose, the images taken with the high speed camera have been averaged vertically. A short series of images taken before ( $>62.5 \mu\text{s}$  before ignition, blue curve on the bottom) and after ignition is shown in Fig. 5.

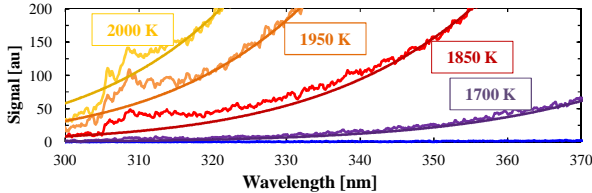


Fig. 5 Measured spectra during combustion: bottom line (blue) just before combustion. Slightly increased line (violet) shortly after combustion.

The smooth curves show the theoretical black body radiation for the indicated temperature. They help to differentiate between the light from soot incandescence and the OH\* chemiluminescence. Even though the averaging of the image tends to further attenuate the weak signal, a contribution of OH radicals can be discerned near 310 nm. In order to substantiate this observation, a LIFBASE [15] simulation has been performed, assuming a temperature of 2000 K and an overall Gaussian line shape of 0.7 nm FWHM. The result of this simulation is shown in Fig. 6, plotted against the observed signal. Whereas the OH\* 1-0 emission at 281/283 nm remains indiscernible, mostly owing to the poor transmission of the spectrometer in this wavelength range, the OH\* emission at 310 nm can be clearly identified in the observed signal, in spite of the strong perturbation by the thermal radiation of soot.

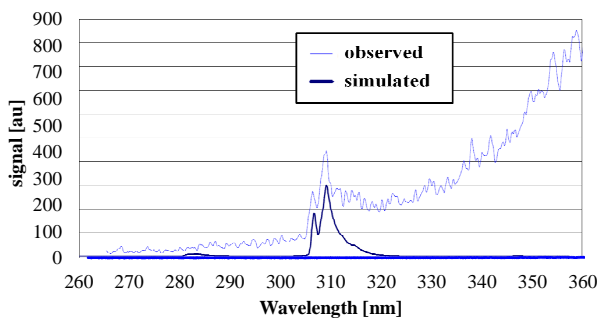


Fig. 6 Observed signal and simulated OH\* emission

The investigation showed that for a combusting diesel spray under the conditions of large two-stroke engines, the OH\* signal cannot clearly be distinguished from the radiation by soot incandescence. Therefore, the setup described earlier (compare Fig. 3) has been used to discern between OH\* chemiluminescence and soot incandescence (as suggested earlier by [16]). A superposition of the two images allows the observation of the OH\* chemiluminescence and the soot incandescence.

Fig. 7 shows sequent single shot images of the back illuminated spray (red) with the superimposed chemiluminescence recording (green). On the left image,  $62.5 \mu\text{s}$  after ignition, several nests can be seen in the UV spectrum. From soot incandescence no light is visible, so far. An image later ( $125 \mu\text{s}$  after ignition), the area containing OH\* has increased significantly. The tip of the OH\* containing area reaches about 20 mm further as on the image before. With a frame rate of 16 kHz this results in a propagation velocity of about 320 m/s. At this time also the first nests with very bright soot have built close to where the combustion started. The third image shows only small areas of OH\* but large areas where soot is burning.

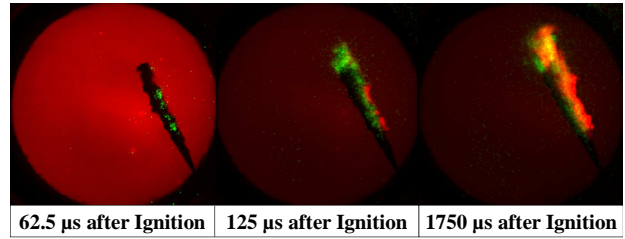


Fig. 7 Sequent single shot recordings of back illuminated images as well as soot incandescence, colored in red and OH\* chemiluminescence visualized in green

Particularly noticeable is the fact that most of the combustion takes place on the right side of the spray. This could be expected as the strong swirl influence created in the SCC and which is characteristic for large marine two-stroke engines, transports the gas phase in this direction. The evaporated fuel is therefore pushed to the side and its mixing with the entrained air enhanced. At the same time, the ignition chemistry in this cloud of evaporated and mixed fuel is proceeding until, finally, actual combustion starts. In a first measurement series, the ignition behavior was investigated for different gas temperatures. Starting from engine-like conditions (gas density:  $33.3 \text{ kg/m}^3$ , gas temperature: 900 K, rail pressure: 100 MPa, injector: coaxial single hole injector with a nozzle hole diameter of 0.875 mm, fuel: light fuel oil. Pertinent to [16]) the temperature was decreased (790 K, 760 K, 730 K) while the gas density was kept constant. For all the different cases, ignition delay, ignition location and flame lift-off have been measured.

The ignition delay between temperatures of 700 K and 810 K was determined by means of an optical fiber probe (Kistler, [13]) recording a global OH\* chemiluminescence signal. For the first series of experiments at high temperature, the probe was not available, yet; therefore, the ignition delay for these cases has been analyzed via the 2-D OH\* chemiluminescence experiments (This results in increased temporal uncertainty of  $\pm 31.25 \mu\text{s}$ ). Fig. 8 shows the ignition delay within the observed temperature range. It is defined as the time between start of injection (the moment the first fuel exits the nozzle) and a significant increase in OH\* signal in the optical probe. The vertical error bars show the standard deviation whereas the horizontal bars show the 1%

measurement error from the temperature signal. As can easily be seen grows the ignition delay drastically towards lower gas temperatures. The main reason for this behavior is the increased time scale of the chemical processes. Due to the lower temperature the evaporation processes becomes also slower but stoichiometric conditions are still provided. Therefore the physical processes are not seen as the limiting factor.

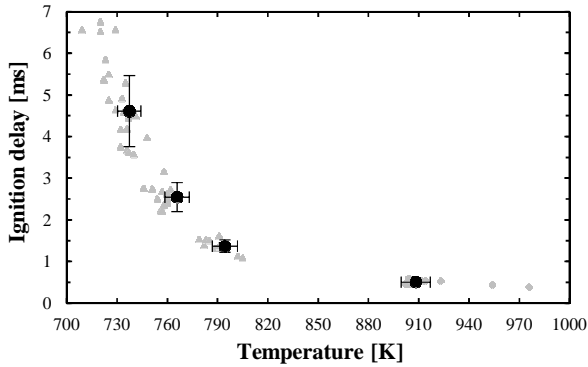


Fig. 8 Ignition delay as a function of gas temperature.

For the investigation of ignition location, the strongest signal intensities have been tracked to define the spot where the fuel ignites. In some cases (~25%), the combustion starts at different locations at about the same time. In case of these simultaneous, separated ignition spots, the average of the different locations was taken. These ignition locations have been measured for each image and the location has been averaged and plotted. As can be seen in Fig. 9, the ignition location is heavily influenced by gas temperature. The visualization shows the averaged back illuminated image of the spray plume. As the density was kept constant, the two phase flow was almost identical for all three temperatures. On top of the spray plume the averaged OH\* chemiluminescence images of the flaming areas 125 $\mu$ s after start of combustion (after the first OH\* was detected) has been plotted. Together with the individual ignition spots for each measurement – the squares plotted on top of the flaming areas – a good impression of the development of the flame. As the ignition delay grows longer with lower temperature, the cloud in which the ignition chemistry is mainly proceeding is transported further downstream so that the ignition location is shifted further away from the nozzle tip. Towards lower gas temperatures the location of the ignition spots becomes unsteady and covers a wider area. Therefore the averaged area of the flaming location as well as the area covered by the ignition spots becomes larger.

This is, on the one hand, due to the increase in size of the cloud as it is penetrating and mixing further. On the other hand, the high dependency from temperature is playing a role, as small deviations within the temperature distribution along the spray have significant influence on the chemical kinetics and therefore on the location where the ignition starts. For all cases the ignition spot is roughly at about half length of spray penetration. With

decreased temperature the location not only moves axially, but also sideways away from the injector axis. Due to the strong swirl which is typical for large two-stroke engines, the ignition spots are carried to the lee side of the spray plume. The swirls bending effect on the gas phase is much stronger compared to the liquid phase, as can also be observed in Fig. 9. The spray deviates only a few millimeters from the injector axis, whereas the ignition locations lie at a significant distance from the injector- and the spray axis.

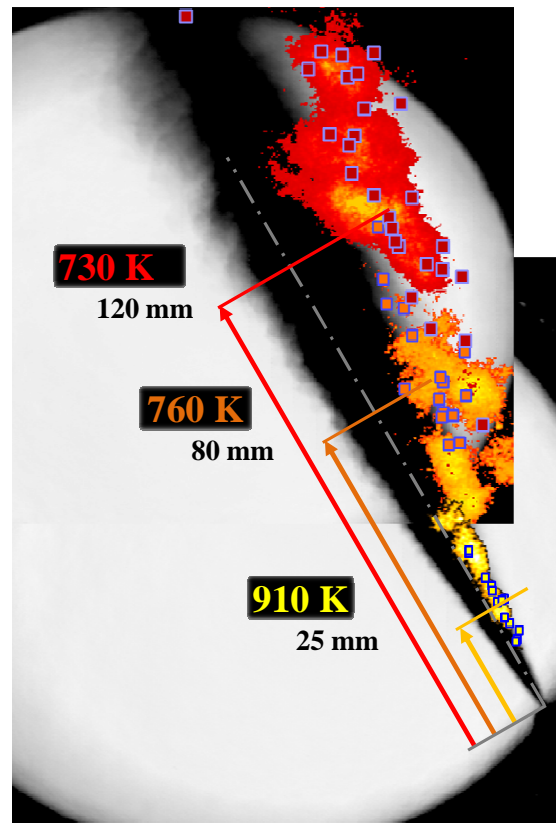


Fig. 9 Averaged image of the UV emitting areas 125  $\mu$ s after start of combustion and ignition spots for different gas temperatures plotted on the averaged back illuminated image of the spray. The indicated distances represent the distance between the corresponding mean spot and the nozzle orifice

To allow comparisons at different temperatures the location of the ignition spots has been defined as the axial distance between nozzle orifice and the averaged location of the individual ignition spot (compare Fig. 9). The mean distances between ignition location and the nozzle tip for all the experiments conducted, have been plotted as a function of temperature as visible in Fig. 10. Similar to the location of the flaming areas shown in Fig. 9, the distance between the orifice and the ignition location is increased. The slower physical and chemical processes leave more time to the evaporating/evaporated fuel to be transported in axial direction. The fact that the ignition location shows a less distinctive increase towards lower temperature than the ignition delay shows a behavior as described in literature, that the transport velocity is not

linear but decreases along with increased spray penetration. As can be seen in Fig. 9 already, the standard deviation is increased with lower gas temperature. This is mostly due to a higher sensitivity to variations in the temperature distribution of the gas phase. Around 730 K a difference of  $\pm 5$  K in temperature results in a variation in ignition delay of  $\pm 1.5$  ms.

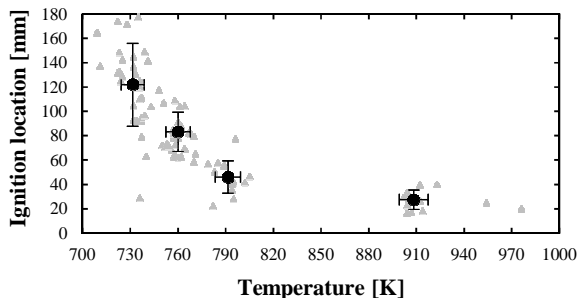


Fig. 10 Distance of ignition location from nozzle tip as a function of gas temperature

Once the fuel is ignited and the pure premixed combustion is over, the flame quickly propagates back towards the nozzle and stabilizes in a statistically stabilized distance to the injector, the so called lift-off height [16]. It was defined as the shortest distance in axial direction between the nozzle orifice and the point where OH\* chemiluminescence reached 10% of the maximum intensity. Figure 11 shows the lift-off as a function of temperature. The increase in distance grows with lower temperatures. At the same time, the standard deviation increases.

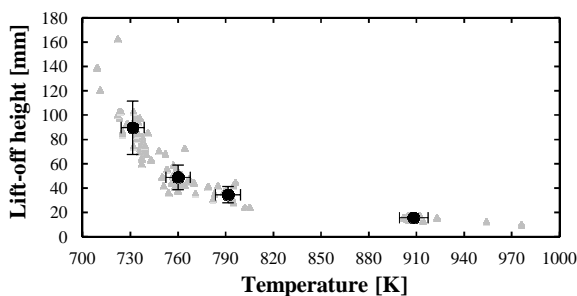


Fig. 11 Flame lift-off as a function of gas temperature

## CONCLUSIONS

In the Spray Combustion Chamber, the flame emission spectrum of a two-stroke marine diesel combustion has been measured at engine-like conditions. It shown that the OH\* signal is masked very early by soot incandescence. This made it necessary to observe both, OH\* chemiluminescence and soot incandescence, simultaneously to distinguish between both UV sources. An appropriately configured setup was used to investigate the ignition delay, ignition location and the lift-off during stable combustion. In parallel, the global OH\* signal was recorded with an optical probe, allowing to measure the ignition delay with higher sampling rate. The results

showed a significant increase in ignition delay as well as in the distances of ignition location and lift-off from the nozzle tip, when lowering gas temperature. At the same time, the standard deviation increases and the location of the ignition becomes more stochastic. This could be expected as earlier measurements for smaller injectors showed similar results [16]. Due to the strong swirl, which is characteristic for large two-stroke engines, the ignition location is always shifted towards the lee side of the spray. Further investigations are planned to include variations in fuel pressure as well as fuel quality.

## Acknowledgements

The present work has been conducted as part of the HERCULES- project within the EC's 7<sup>th</sup> Framework Program, Contract SCP7-GA-2008-217878. Financial support by the Swiss Federal Government (SER & SFOE) Contract 154269, Project 103241) is gratefully acknowledged.

## REFERENCES

- [1] IMO, Annex VI of MARPOL 73/78, "Regulations for the Prevention of Air Pollution from Ships and NOx Technical Code", EA664E, London, 2009
- [2] Hensel S., et. al, submitted to COMODIA, Fujioka, Japan (2012)
- [3] Herrmann K., Schulz R., and Weisser G, CIMAC Congress, Vienna, Austria, 2007, No. 98
- [4] Kyrtatos N.P., Kleimola M., Marquard R., CIMAC Congress, Vienna, Austria, 2007, No. 31
- [5] Herrmann K., von Rotz B., Schulz R., and Weisser G, ISME 2011, Kobe, Japan, 2011
- [6] Herrmann K., von Rotz B., Schulz R., Weisser G., Boulouchos K., and Schneider B., ILASS-Europe 2010, Brno, Czech Republic, 2010
- [7] von Rotz, B., Herrmann, K., Weisser, G., Cattin, M., Bolla, M., and Boulouchos, K., ILASS-Europe 2011, Estoril, Portugal, 2011
- [8] Bolla M., Cattin M.A., Wright Y.M., Boulouchos K., and Schulz R., ASME, Torino, Italy, 2012, ICES2012-81016
- [9] Gaydon A.G., The Spectroscopy of Flames, Chapman and Hall, London, 1974
- [10] Dec J.E., and Espey C., SAE 982685, 1998
- [11] Herrmann K., et al. ICLASS, Vail, USA, 2009
- [12] Schneider B., PhD thesis, No. 15004, ETH Zürich, 2003
- [13] KTI-Projekt 10604, Schlussbericht, Vögelin Ph., Bertola A., Obrecht P., Boulouchos K. 2011
- [14] Schmid A., von Rotz B., Internal Report "Setup for Chemiluminescence with Optical Probes" 2012
- [15] J. Luque and D.R. Crosley, "LIFBASE: Database and spectral simulation (version 1.5)", SRI International Report MP 99-009 (1999)
- [16] Picket L.M., Siebers D.L., Journal of Engineering for Gas Turbines and Power, 127:187-196 (2005).